AD-A129 822 CHARACTERIZATION OF SILICON GROWN BY COLD CRUCIBLE TECHNIQUES(U) AIR FORCE WRIGHT AERONAUTICAL LABS WRIGHT-PATTERSON AFB OH D W FISCHER ET AL. APR 83 1/1

UNCLASSIFIED AFWAL-TR-83-4015 F/G 20/2 NL

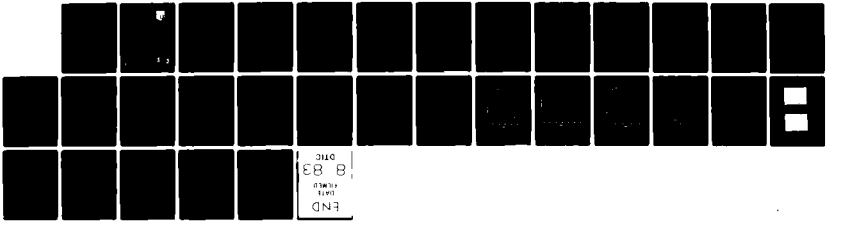

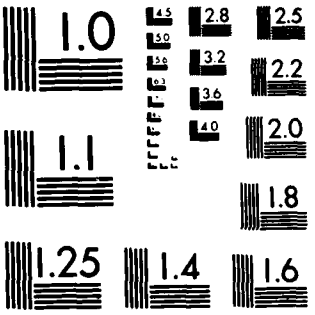

MICROCOPY RESOLUTION TEST CHART
NATIONAL BUREAU OF STANDARDS-1963-A

AFWAL-TR-83-4015

CHARACTERIZATION OF SILICON GROWN BY COLD CRUCIBLE TECHNIQUES

David W. Fischer
John J. Rome
Timothy L. Peterson
Melvin C. Ohmer

Laser & Optical Materials Branch
Electromagnetic Materials Division

April 1983

Interim Technical Report for Period January 1981 - September 1982

MATERIALS LABORATORY
AIR FORCE WRIGHT AERONAUTICAL LABORATORIES
AIR FORCE SYSTEMS COMMAND
WRIGHT-PATTERSON AIR FORCE BASE, OHIO 45433

NOTICE

When Government drawings, specifications, or other data are used for any purpose other than in connection with a definitely related Government procurement operation, the United States Government thereby incurs no responsibility nor any obligation whatsoever; and the fact that the government may have formulated, furnished, or in any way supplied the said drawings, specifications, or other data, is not to be regarded by implication or otherwise as in any manner licensing the holder or any other person or corporation, or conveying any rights or permission to manufacture use, or sell any patented invention that may in any way be related thereto.

This report has been reviewed by the Office of Public Affairs (ASD/PA) and is releasable to the National Technical Information Service (NTIS). At NTIS, it will be available to the general public, including foreign nations.

This technical report has been reviewed and is approved for publication.

David W. Fischer

DAVID W. FISCHER, Project Engineer

G. Edward Kuhl

G. EDWARD KUHL, Chief
Laser and Optical Materials Branch
Electromagnetic Materials Division

FOR THE COMMANDER

M. L. Minges, Chief
Electromagnetic Materials Division

"If your address has changed, if you wish to be removed from our mailing list, or if the addressee is no longer employed by your organization please notify AFWAL/MLPO, W-PAFB, OH 45433 to help us maintain a current mailing list".

Copies of this report should not be returned unless return is required by security considerations, contractual obligations, or notice on a specific document.

UNCLASSIFIED

SECURITY CLASSIFICATION OF THIS PAGE (When Data Entered)

REPORT DOCUMENTATION PAGE		READ INSTRUCTIONS BEFORE COMPLETING FORM
1. REPORT NUMBER AFWAL-TR-83-4015	2. GOVT ACCESSION NO. AD-A129822	3. RECIPIENT'S CATALOG NUMBER
4. TITLE (and Subtitle) CHARACTERIZATION OF SILICON GROWN BY COLD CRUCIBLE TECHNIQUES		5. TYPE OF REPORT & PERIOD COVERED Interim Technical Report Jan 1981 - Sep 1982
		6. PERFORMING ORG. REPORT NUMBER
7. AUTHOR(s) David W. Fischer, John J. Rome, Timothy L. Peterson, and Melvin C. Ohmer		8. CONTRACT OR GRANT NUMBER(s)
9. PERFORMING ORGANIZATION NAME AND ADDRESS Materials Laboratory (AFWAL/MLPO) Air Force Wright Aeronautical Laboratories, AFSC Wright-Patterson Air Force Base, OH 45433		10. PROGRAM ELEMENT, PROJECT, TASK AREA & WORK UNIT NUMBERS Program Element 61102F Project 2306 Task 2306Q1 Work Unit 23060106
11. CONTROLLING OFFICE NAME AND ADDRESS Materials Laboratory (AFWAL/MLP) Air Force Wright Aeronautical Laboratories, AFSC Wright-Patterson Air Force Base, OH 45433		12. REPORT DATE April 1983 13. NUMBER OF PAGES 31
14. MONITORING AGENCY NAME & ADDRESS(if different from Controlling Office)		15. SECURITY CLASS. (of this report) UNCLASSIFIED 15a. DECLASSIFICATION/DOWNGRADING SCHEDULE

16. DISTRIBUTION STATEMENT (of this Report)

Approved for public release; distribution unlimited.

17. DISTRIBUTION STATEMENT (of the abstract entered in Block 20, if different from Report)

18. SUPPLEMENTARY NOTES

19. KEY WORDS (Continue on reverse side if necessary and identify by block number)

Silicon, absorption spectra, infrared absorption, Hall effect, cold crucible growth.

20. ABSTRACT (Continue on reverse side if necessary and identify by block number)

Single crystal silicon grown by the cold crucible technique has been characterized by Fourier transform infrared (FTIR) spectroscopy, Hall effect, and etching. Boron, phosphorus, carbon, and oxygen were the only impurities observed. At 10K, FTIR data indicated oxygen concentrations in the low- to mid- $10^{15}/cm^3$ range and carbon concentrations in the mid-10^{16} to low $10^{17}/cm^3$ range. Absorption and Hall data are in close agreement on the boron concentration (low $10^{15}/cm^3$) which seems to be significantly higher in the cold crucible

DD FORM 1 JAN 73 1473 EDITION OF 1 NOV 65 IS OBSOLETE

UNCLASSIFIED

SECURITY CLASSIFICATION OF THIS PAGE (When Data Entered)

crystals than in the poly-crystalline silicon starting material. This indicates that boron is being added during the growth process. The oxygen concentration in the cold crucible material is significantly lower than in conventional Czochralski-grown material. The Hall mobility of the cold crucible samples is in the normal range (315-350 cm^2/volt-sec), the resistivity varied from about 12 to 22 ohm-cm and the defect density was high (~~$>10^3$~~). Further development of cold crucible growth technique is recommended.

FOREWORD

This report describes an in-house study conducted by personnel of the Laser and Optical Materials Branch, Electromagnetic Materials Division, Materials Laboratory, Air Force Wright Aeronautical Laboratories, Wright-Patterson Air Force Base, Ohio 45433 under Project No. 2306, Task No. 2306Q1, Work Unit 2306Q106. The report covers work performed during the period January 1981 to September 1982. The report was released by the authors on 15 November 1982.

The authors wish to thank Mr. Robert C. Marshall of the Rome Air Development Center (RADC/ESM) for his helpful suggestions and participation in defining this cooperative program between AFWAL and RADC. We also thank Mr. David A. Walsh and Mr. Robert Bertke of the University of Dayton Research Institute for the sample cutting and polishing.

TABLE OF CONTENTS

SECTION		PAGE
I.	INTRODUCTION	1
II.	EXPERIMENTAL RESULTS	4
	1. Infrared Absorption	4
	2. Hall Data	6
	3. Etching	9
	4. Other Data	10
III.	CONCLUSIONS AND RECOMMENDATIONS	11
	REFERENCES	12

LIST OF ILLUSTRATIONS

FIGURE		PAGE
1.	Infrared Absorption Spectrum of Cold Crucible Sample 0226-663-0825 Showing Boron and Carbon Lines.	13
2.	Infrared Absorption Spectra of Cold Crucible Sample Showing Kolbesen Effect.	14
3.	Typical Carbon Infrared Absorption Line Observed in Cold Crucible Samples.	15
4.	Typical Oxygen Infrared Absorption Line Observed in Cold Crucible Samples.	16
5.	One Level Fit of Carrier Concentration Data vs. 1000/T for Sample 0227-667-0828.	17
6.	Comparison of Types of Defects Observed in Crystal 1 and Crystal 6 After Wright Etching.	18

LIST OF TABLES

TABLE		PAGE
1.	Future Silicon Material Requirements Compared to Typical Current Material.	19
2.	Lower Detection Limits in FTIR Spectroscopy for Impurities in Silicon (T 20°K).	19
3.	FTIR Results for Some Cold Crucible Silicon Samples and Poly Silicon Starting Materials.	20
4.	Some Published Values of IR Absorption Calibration Factors for Oxygen in Silicon.	21
5.	Hall Results for Cold Crucible Silicon Samples.	22
6.	Resistivity and Hall Mobility at 300K for Cold Crucible Silicon Samples.	22
7.	Defect Densities in Cold Crucible Silicon Samples.	23

SECTION I

INTRODUCTION

The U.S. Air Force has a strong interest in silicon as a semiconductor material for electronic device and infrared detector applications. To meet future requirements, better quality bulk silicon is needed.

All of the single crystal silicon currently used for semiconductor applications is grown by one of two techniques: the Czochralski (CZ) technique or the Floating-Zone (FZ) technique. The CZ technique involves pulling a single crystal from the melt which is contained in a quartz crucible. The FZ technique makes use of induction heating and zone melting of a supported polycrystalline silicon rod which eliminates the need for a containment crucible. By far the majority of single crystal silicon in use today is grown by the CZ technique. Unfortunately, neither growth technique yields silicon crystals capable of meeting future requirements for purity, perfection or processability. Improvements are needed in bulk resistivity, minority carrier lifetime, and concentration control and uniformity for impurities and defects. Some silicon material property goals (future requirements) are compared to typical properties obtained from currently available CZ and FZ material in Table 1.

CZ crystals can be grown to large size and made virtually dislocation-free. The main problem with this material is the residual impurity concentration. Since the melt is in contact with a quartz crucible, some reaction and impurity leaching will occur. The primary impurities found in the resultant crystals are oxygen and carbon but other elements such as boron, phosphorus, and aluminum may also be present in sufficient quantity to cause degradation of important properties.

FZ grown crystals tend to be of higher purity than CZ material because the melt does not come in contact with a crucible. Unfortunately, lack of bulk homogeneity (property uniformity throughout the crystal) is a problem. Another problem for some applications is the low oxygen concentration.

The oxygen concentration, in fact, is a significant factor in the quest for better bulk silicon for device application. On the one hand it has been shown that a high oxygen content directly correlates with a high defect density which makes the material unsuitable for certain applications such as VLSI. On the other hand, it has also been shown that the oxygen concentration must be maintained above a certain level ($\sim 10^{18} cm^{-3}$) for optimum wafer processability (minimum wafer warpage). It is thought that oxygen precipitates act as getters for defects and help insure a higher device yield. This is the main reason that FZ material with its low oxygen concentration is usually not acceptable for device applications. What is needed, therefore, is a bulk silicon material in which the oxygen concentration and uniformity can be carefully controlled while all other impurities are kept to a minimum such that the requirements listed in Table 1 can be met.

A process which appears to have good potential for the growth of ultrapure silicon possessing the requisite properties is the cold crucible (skull-melting) technique. In this technique, a molten column of silicon is confined in a water-cooled cold-crucible structure and is squeezed and is squeezed radially and contained by an RF field. The base of the molten column is supported on the unmelted portion of the feed material so that while the melt is physically supported it is not in contact with any contaminating solid (Reference 1). A crystal can then be pulled from the melt similar to the manner in which it is done in a standard CZ process. Impurity contamination such as occurs from the crucible in conventional CZ growth should be significantly reduced. Furthermore, it should be possible to more accurately control and maintain the oxygen concentration at whatever level is desired for optimum material processability.

In light of the potential advantages of the cold crucible growth process, Rome Air Development Center (RADC/ESM) at Hanscom AFB, MA initiated a contract with Ceres Corporation of Waltham, MA (Contract #F19628-80-C-0104). The objective of the program was to explore the feasibility of utilizing a cold crucible system for the growth of high purity, oxygen-free single crystals of silicon (Reference 1). During

the program, numerous crystal growths were made to evaluate and improve the process. RADC needed a means of assessing the quality of the crystals as they were grown. As a result of this need, an informal cooperative agreement between RADC/ESM and AFWAL/MLPO was initiated. We at AFWAL/MLPO (WUD#48) are heavily involved in an in-house research effort on the properties of silicon-based materials for both detector and device applications and so we had a strong interest in this RADC/Ceres contract. Under the informal agreement, RADC sent us pieces of silicon boules grown under the contract and we performed characterization analyses on them. The specific analyses performed were Fourier Transform Infrared (FT spectroscopy, Hall effect and etching. Fewer samples than anticipa were received. This report summarizes the characterization results r those samples.

SECTION II

EXPERIMENTAL RESULTS

1. INFRARED ABSORPTION

Samples for infrared absorption analysis were prepared in our laboratory from boule sections submitted to us by RADC/ESM. All samples were cut to 4mm thickness and both faces were polished. The samples were cooled to $10^{o}K$ in either a liquid helium optical dewar or a Lake Shore Cryogenics model LTS-21-D70C closed cycle refrigeration system.

All spectra were recorded at a resolution of 1 cm^{-1} using a Digilab model FTS-20CVX Fourier transform spectrophotometer purged with dry nitrogen. The spectrophotometric arrangement, which included a cesium iodide (CsI) beamsplitter and TGS detector with a CsI window, permitted investigation in the 4000 to 200 cm^{-1} region. The data were recorded in the single beam mode with the sample transmittance referenced to an empty sample holder. Transmittance was then converted to absorption coefficient in the usual way.

The purpose of the FTIR analysis was to determine the concentration of impurities in the samples. Impurities of particular interest were oxygen, carbon, and boron plus anything else that might be detected. Oxygen and carbon in silicon give rise to local mode vibrations at 1136 cm^{-1} and 607 cm^{-1}, respectively (if the sample temperature is about $10^{o}K$) (References 2, 3). Boron and phosphorus (and also the other group III acceptors and group V donors), on the other hand, form electronic energy states within the silicon band gap which give rise to a series of discrete excitation lines in various infrared spectral regions (References 4, 5, 6). Optimum detectability for each of these impurities occurs when the sample is cooled to near liquid helium temperatures. Approximate lower limits of detectability of some of these impurities in silicon are given in Table 2. The only impurities detected by FTIR in the cold crucible samples were carbon, oxygen, boron, and phosphorus.

A portion of a typical scan from one of these samples is shown in Figure 1. The carbon peak is seen at 607 cm^{-1} and the other peaks are

the excitation lines of boron. In theory, the intensity of a peak should be directly proportional to the concentration of the impurity giving rise to that peak. By measuring the integrated intensity (peak area) and multiplying it by an empirically determined calibration factor the impurity concentration can be determined (Reference 7).

Table 3 lists the impurity concentrations determined for the cold crucible samples and for two samples of polycrystalline silicon. The polycrystalline silicon is used as the starting material in the cold crucible crystal growth (Reference 1). Notice that most of the cold crucible samples have considerably more boron in them than the poly silicon starting material. One of the boules also had a measurable amount of phosphorus in it as shown in Figure 2. Normally the phosphorus is overcompensated by the boron but by using additional band-gap light pumping (also called Kolbesen excitation) (Reference 8) the phosphorus becomes infrared active. A small quartz-halogen incandescent bulb is used for the band-gap pumping and the results are clearly evident in Figure 2. The bottom spectrum was obtained with the light off (no Kolbesen excitation) and shows only lines due to boron. The top spectrum was obtained with the light turned on (everything else remained unchanged) and now, in addition to the boron lines, three new lines appear. All three of these new lines are due to phosphorus. Its concentration is estimated to be about $10^{13}cm^{-3}$. Only the samples from boule #93 showed evidence of phosphorus.

Another common impurity in silicon is carbon. As can be seen in Table 3, all samples contained a measurable amount of carbon. It appears that one of the later boules (#93) contains even less carbon that the poly-Si starting material. The other crystal samples contain a bit more. A typical carbon spectrum from one of the samples is shown in Figure 3. Carbon has one of the poorest detectability limits of all the infrared-active impurities in silicon because it lies on top of a strong silicon two-phonon lattice band (Table 2). Careful spectral differencing between the sample spectrum and the silicon lattice spectrum must be performed to obtain an accurate absorption coefficient. There is considerable disagreement among various investigators as to the correct calibration

factor to use for determining the carbon concentration (Reference 10) as indicated in Table 4. Different sample temperatures and different instrumental conditions contribute to the disagreement but another important factor is the difficulty in obtaining reliable silicon standards with accurately known amounts of carbon. We plan to investigate this problem in more detail in the near future. In the meantime we are using Honeywell's calibration factor (Reference 7) because it is one of the few determined at near liquid helium temperature using an FTIR instrument similar to ours.

The oxygen situation is even worse than carbon. There is a similar disagreement among various workers on the IR absorption calibration factor (Table 4), partly for the same reasons as given above for carbon. In addition, there is one serious complicating factor. The peak at 1136 cm^{-1} (at $10^{o}K$) such as shown in Figure 4, arises only from the oxygen which is in interstitial lattice sites. Not all of the oxygen need be in such O_i sites. It is well known that oxygen can and does form precipitates and complexes with other impurities and defects in which case it does not contribute to the 1136 cm^{-1} line. So the 1136 cm^{-1} line does not indicate the total oxygen concentration, but only the interstitial oxygen concentration. These points should be kept in mind when evaluating the oxygen values listed in Table 3. They were determined from the absorption coefficient of the 1136 cm^{-1} line using Honeywell's calibration factor (Reference 7). Nevertheless, it is clear that the cold crucible grown crystals contain considerably less oxygen than standard CZ grown crystals. Conventional CZ silicon crystals usually have oxygen in the mid-10^{17} to 10^{18} concentration range, probably due to reaction of the molten silicon with the quartz crucible.

2. HALL DATA

Samples for electrical transport measurements were prepared from wafers cut from boule sections submitted to this laboratory by RADC/ESM. These wafers were cut immediately adjacent to other wafers cut for infrared absorption analysis. The wafers were nominally 0.5 mm thick, and both faces were polished. Cloverleaf samples were then cut from these wafers for Hall effect analysis by the method of van der Pauw (Reference 11).

The purpose of the Hall effect measurements was to determine the identity and concentration of electrically active impurities in the samples. These measurements were made at temperatures from about 20K to 380K. From these measurements, the temperature dependence of the carrier concentration, as well as the resistivity and Hall mobility, were determined.

The carrier concentration was calculated from the Hall effect measurements using the relationship

$$P = \frac{1}{R_H e} \tag{1}$$

where p is the carrier concentration, e is the electronic charge, and R_H is the Hall coefficient given by

$$R_H = \frac{R^+ - R^-}{2} \frac{t}{B} \tag{2}$$

In Equation 2 R^+ and R^- is the Hall voltage divided by the Hall current for a magnetic field of magnitude B in a positive and negative direction respectively.

$$p + N_D = \sum_i \frac{N_{A_i}}{1 + p(g_i/N_V) \exp (E_{A_i}/kT)} \tag{3}$$

where N_V is the density of states in the valence band and is given by

$$N_V = \frac{2(2\pi m^* T)^{3/2}}{h^3} \tag{4}$$

where N_{Ai}, E_{Ai}, and g_i are the concentration, ionization energy, and ground state degeneracy, respectively, of the i^{th} acceptor, p is the carrier concentration, k is Boltzmann's constant, T is the temperature in degree kelvin, h is Planck's constant, and $m^*(T)$ is the carrier concentration effective mass. An analytical expression (Reference 12)

for m*(T) obtained in AFWAL/MLPO was used in this analysis. N_D is the net donor concentration and is given by

$$N_D = \sum_i N_{D_i} - \sum_i N_{D_j} \quad , \qquad (5)$$

where N_{Di} are all donor levels and N_{Aj} are all acceptor levels which are overcompensated and do not contribute to the measured carrier concentration, that is, they are below the Fermi level and remain fully ionized at all temperatures. This analysis yields the impurity concentration and activation energy for each acceptor species that is uncompensated by residual donors, or that is not overcompensated by more than a factor of $2N_A$.

In each of the cold crucible samples only one acceptor level was observed, and that acceptor was identified as boron. The carrier concentration data as a function of 1000/T shown in Figure 5 are typical of all of the samples. A one level computer fit to the data is also shown in this figure as a solid line. The activation energy determined from this fit was .0450 eV, thus identifying the impurity as boron.

The impurity concentrations as determined by the Hall analysis for these cold crucible samples are listed in Table 5. The concentration of boron in crystals 1 and 2 was about $7 \times 10^{14} cm^{-3}$. The four crystals grown subsequently contained about two times that amount of boron (1.3×10^{15} atoms/cm^3). The concentrations of boron determined by Hall analysis agreed quite well with those determined by infrared absorption listed in Table 3.

The resistivity and Hall mobility of the cold crucible crystals were also measured using van der Pauw type Hall samples. The resistivity at 300K is indicative of the concentration of the Major dopant impurity. Measuring the resistivity in different directions is also a useful tool for determining the homogeneity of the material. The mobility is the velocity of a charge per unit electric field and is strongly dependent upon the purity of the material, temperature, and the crystalline quality.

Values of the resistivity and the Hall mobility at 300K are listed in Table 6. Measurements of resistivity in different directions were nearly equal and did not indicate any problems with nonuniformity in these samples. The Hall mobility was approximately the same from one sample to the next. The Hall mobility at 300K for a boron doped conventional Czochralski silicon sample with a net donor concentration of 3.4×10^{13} cm^{-3} and a boron concentration of 2.4×10^{15} cm^{-3} has been determined to be 326 cm^2/volt-sec. The mobilities for the cold crucible samples were of the same magnitude. It is therefore concluded that the crystal quality of these samples, at least in terms of its effect on mobility, is comparable to the quality in conventionally grown crystals.

3. ETCHING

Defects such as dislocations in silicon are known to have a deleterious effect on its electrical properties, particularly carrier lifetime. Therefore, wafers from each crystal of cold crucible silicon submitted to this laboratory by RADC/ESM were preferentially etched to reveal the defects present. Wafers were etched for ten minutes in Wright etch at room temperature (Reference 13). Etched wafers were then examined microscopically. Micrographs at 116X taken at several locations across the wafer surface were used to determine the average defect density.

The results of the defect studies are tabulated in Table 7. It can be seen that all of these crystals had a large defect density. Most of the defects in the two early crystals, numbers 1 and 2, were dislocations although some stacking faults and shallow etch pits were also observed. In the four subsequent crystals, more stacking faults than dislocations were generally observed.

Figure 6 illustrates the differences in defects observed in the crystals. Figure 6(a) is typical of crystals 1 and 2 and shows mostly dislocation etch pits. Figure 6(b) is typical of crystals 3 through 6 and shows many stacking faults and shallow etch pits in addition to the dislocation etch pits. The triangular shape of the dislocation etch pits observed for each of these crystals indicates that the orientation of these crystals was (111).

4. OTHER DATA

The personnel of RADC/ESM also submitted some of their samples to Manlabs, Inc. for analysis. One of their analyses involved determination of the total carbon and oxygen content using a LECO combustion-type apparatus. The average data for their measurements on two of the samples were:

	Carbon	Oxygen
Polycrystalline Sample	72ppm	22ppm
Cold Crucible Crystal	140ppm	18ppm

These values are considerably higher than our FTS values listed in Table 3 and also seem unreasonably high in view of what is known about typical impurity concentrations expected for average quality polycrystalline silicon. We don't know enough about the combustion-type analysis used in this case to make specific comments about it but we must question the accuracy of the values reported above.

Two different spark source mass spectrographic analyses were also made, one by Manlabs, Inc., the other by Charles Evans and Associates. The results were listed in the cold crucible program contract report (Reference 1) but are not listed here. Some of the results seemed very strange and questionable to us. In our experience mass spec data on samples such as these can be very unreliable unless they are run on an instrument dedicated solely to silicon samples because of instrument "memory" effects.

SECTION III

CONCLUSIONS AND RECOMMENDATIONS

From the characterization analyses performed on the cold crucible samples as discussed in the previous sections, the following conclusions are offered:

1) The cold crucible samples have significantly lower oxygen concentration than conventional CZ crystals but somewhat more than the poly-Si starting material.

2) The cold crucible samples have a significantly higher boron concentration than the poly-Si starting material. This would indicate that somehow boron is being added during the growth process.

3) The carbon concentration for one of the cold crucible boules (#93) is a little lower than the poly-Si and the other samples are a little higher but it appears that no significant amount of carbon is added during growth.

4) The Hall mobility of the cold crucible samples is comparable to that measured for conventionally grown silicon crystals.

5) The total defect density, consisting of the dislocation density and stacking faults, is rather high (mid 10^3 or more).

It is recommended that further development work be done on the cold crucible growth technique. From the results obtained so far, it appears that this technique has the potential for producing high quality silicon for detector and electronic device applications. Reasonably good control of oxygen and carbon contamination has been demonstrated but improvements are needed in terms of lower defect density and boron concentration. The cause of the high boron concentration needs to be determined. From the point of view of AFWAL/MLPO, the main emphasis should be directed to the growth of boules which will yield high quality processable silicon wafers for device applications. Recommended material specifications include a resistivity of 200-500Ω-cm, a minority carrier lifetime in the range of 500 microseconds, uniform specifiable oxygen concentrations in the 10 to 40 ppm range and a carbon concentration of less than 0.5 ppm.

REFERENCES

1. J. F. Wenckus and W. P. Menashi, RADC-TR-81-280, Technical Report on RADC Contract F19628-80-C-0104, Oct 1981.

2. J. A. Baker, Solid-State Electronics 13, 1431 (1970).

3. R. C. Newman and R. S. Smith, J. Phys. Chem. Solids 30, 1493 (1969).

4. E. Burstein, G. Picus, B. Henvis, and R. Wallis, J. Phys. Chem. Solids, 1, 65 (1956).

5. A. Onton, P. Fisher, and A. K. Ramdas, Phys. Rev. 163, 686 (1967).

6. R. L. Aggarwal and A. K. Ramdas, Phys. Rev. 140, A1246 (1965).

7. C. E. Jones, D. Schafer, W. Scott, and R. J. Hager, J. Appl. Phys. 52, 5148 (1981).

8. B. O. Kolbesen, App. Phys. Lett. 27, 353 (1975).

9. K. Graff, E. Grallath, S. Ades, G. Goldback, and G. Tolg, Solid-State Electronics 16, 887 (1973).

10. D. H. Brown, J. A. Detrio, R. J. Harris, S. R. Smith, F. Szmulowicz, and D. A. Walsh, AFWAL-TR-81-4157, Final Report on Contract F33615-78-C-5064, Dec 1981.

11. L. J. van der Pauw, Phil. Res. Rep. 13, 1 (1958).

12. J. E. Lang, F. L. Madarasz, and P. M. Hemenger, J. Appl. Phys. 52, 464 (1981).

13. M. W. Jenkins, J. Electrochem. Soc. 124, 757 (1977).

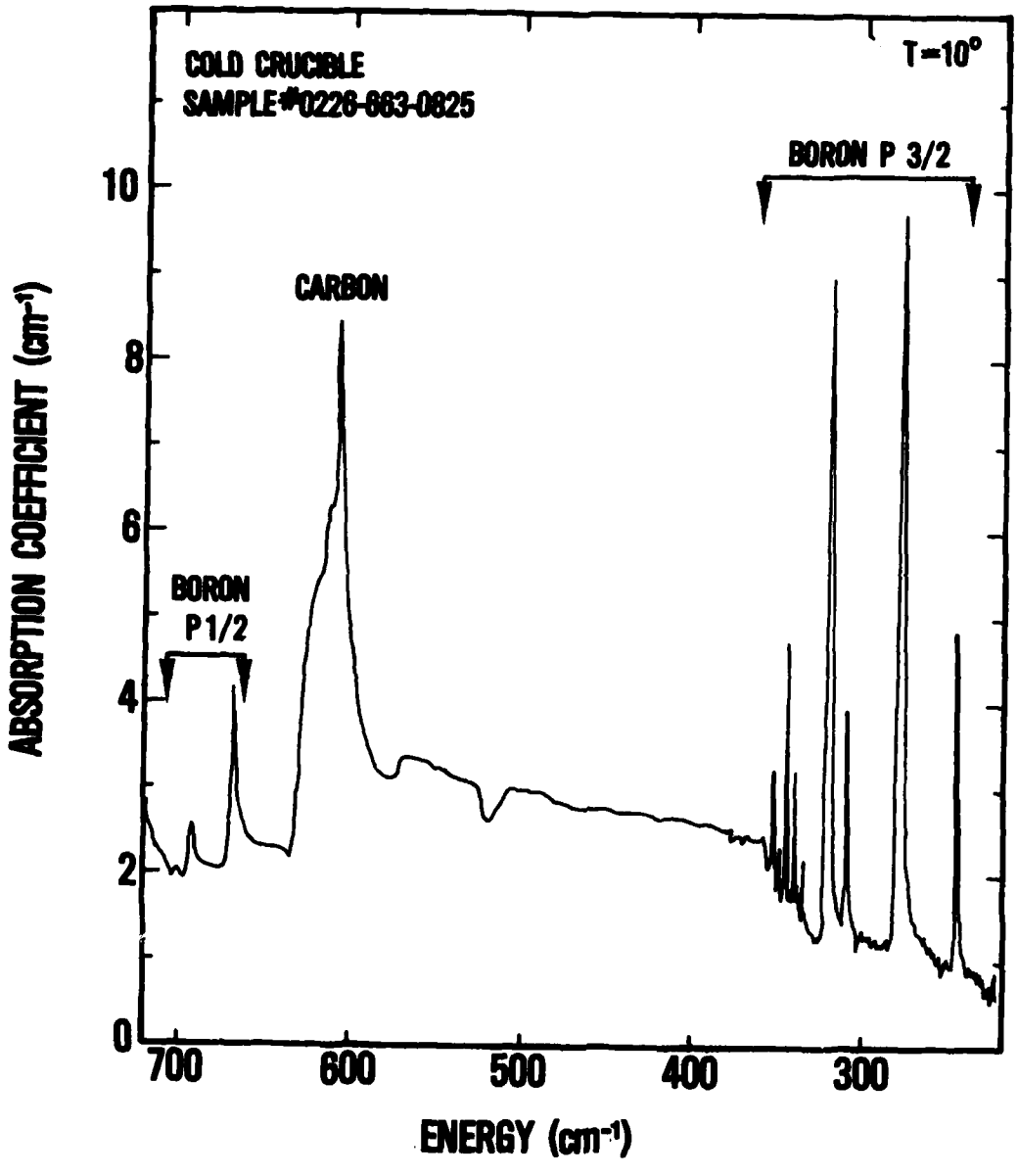

Figure 1. Infrared Absorption Spectrum of Cold Crucible Sample 0226-663-0825 Showing Boron and Carbon Lines.

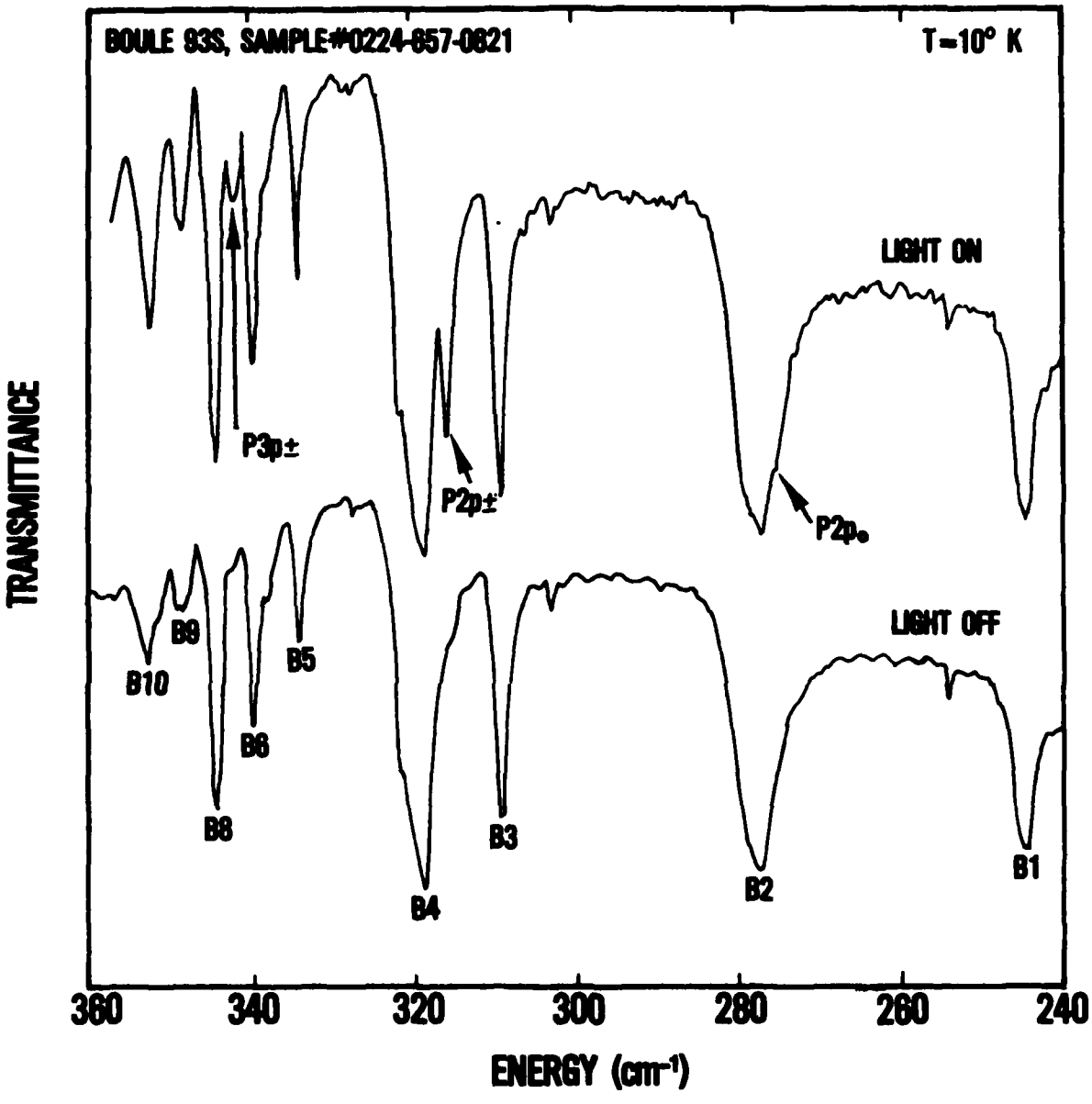

Figure 2. Infrared Absorption Spectra of Cold Crucible Sample Showing Kolbesen Effect.

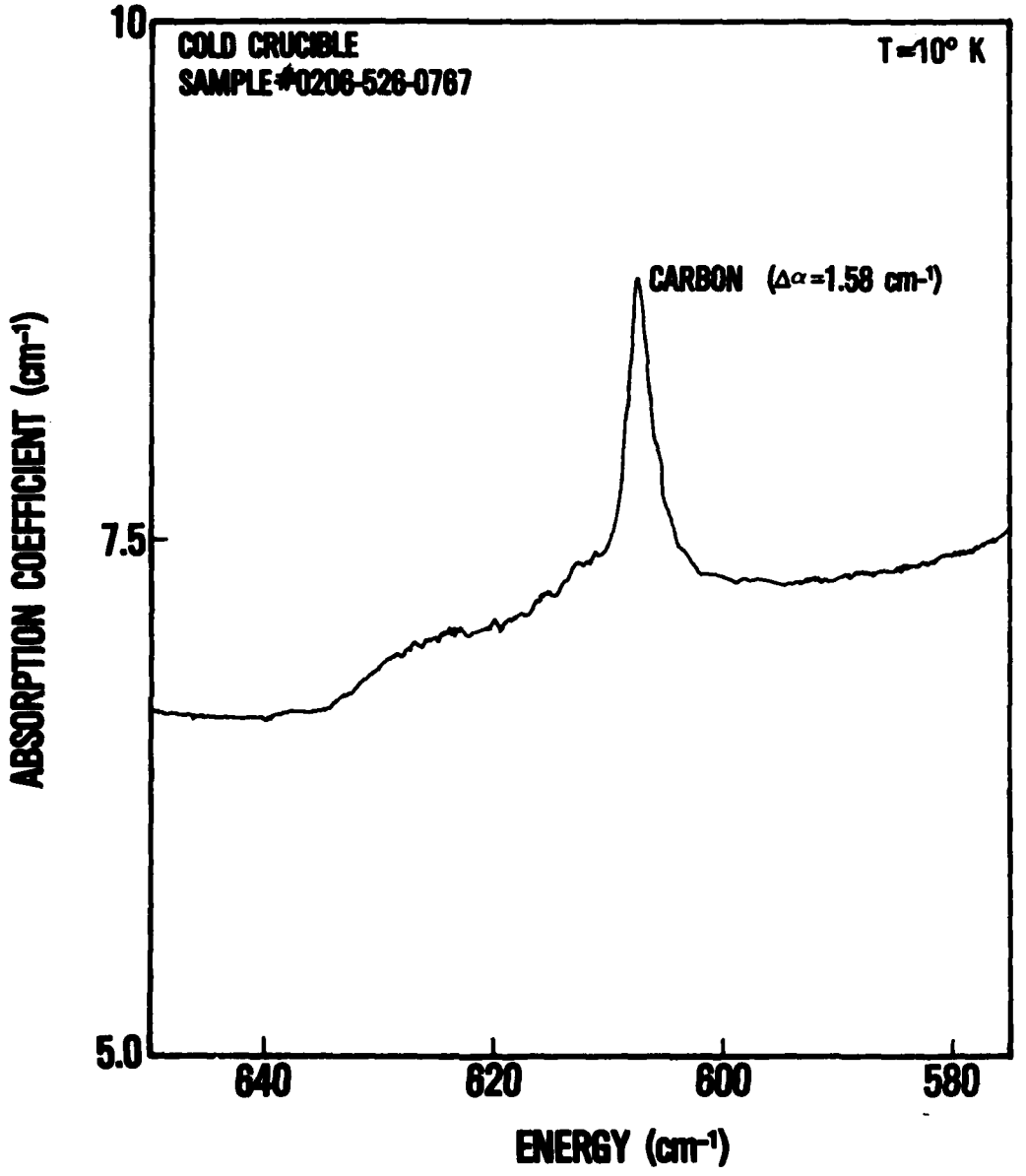

Figure 3. Typical Carbon Infrared Absorption Line Observed in Cold Crucible Samples.

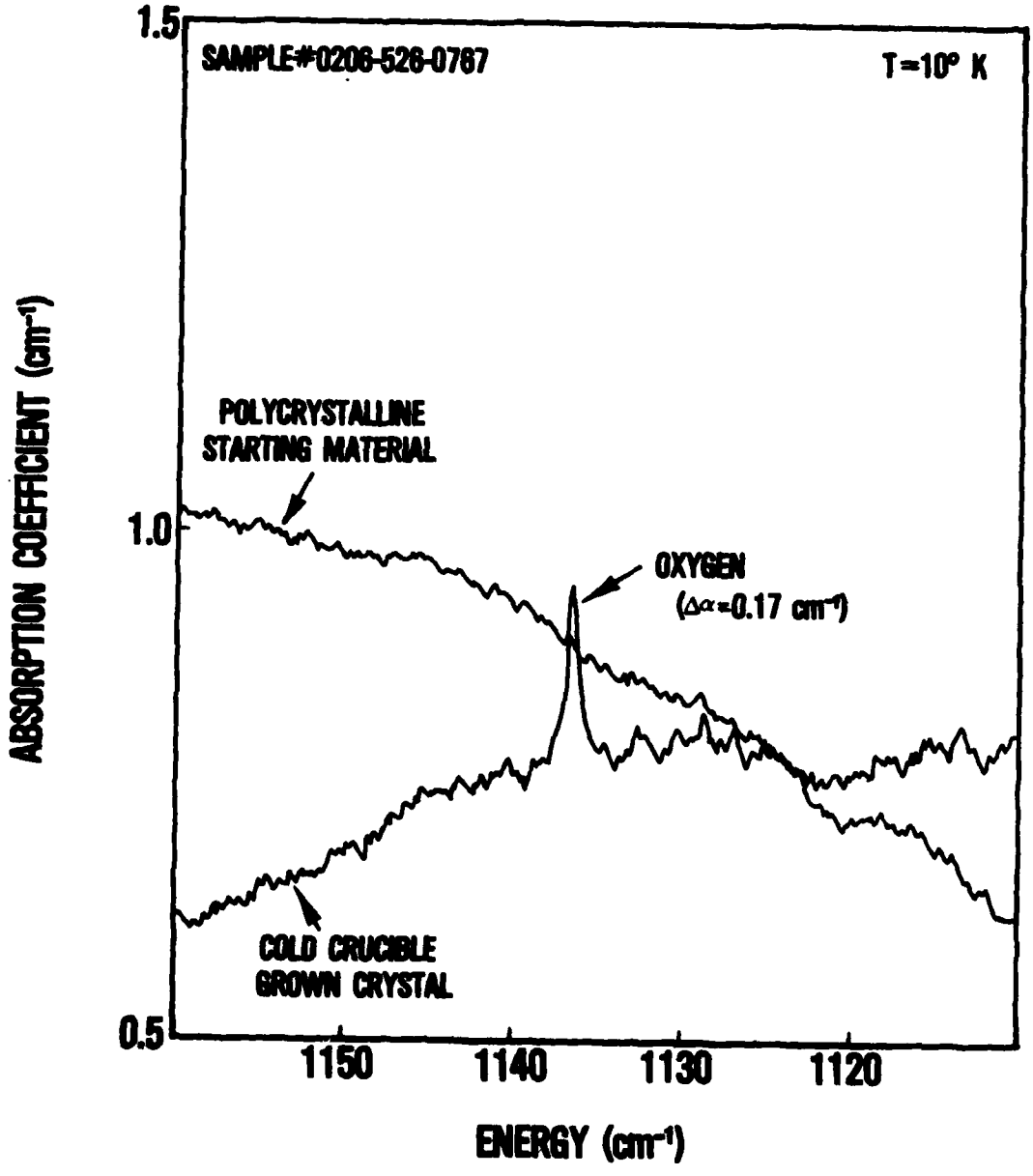

Figure 4. Typical Oxygen Infrared Absorption Line Observed in Cold Crucible Samples.

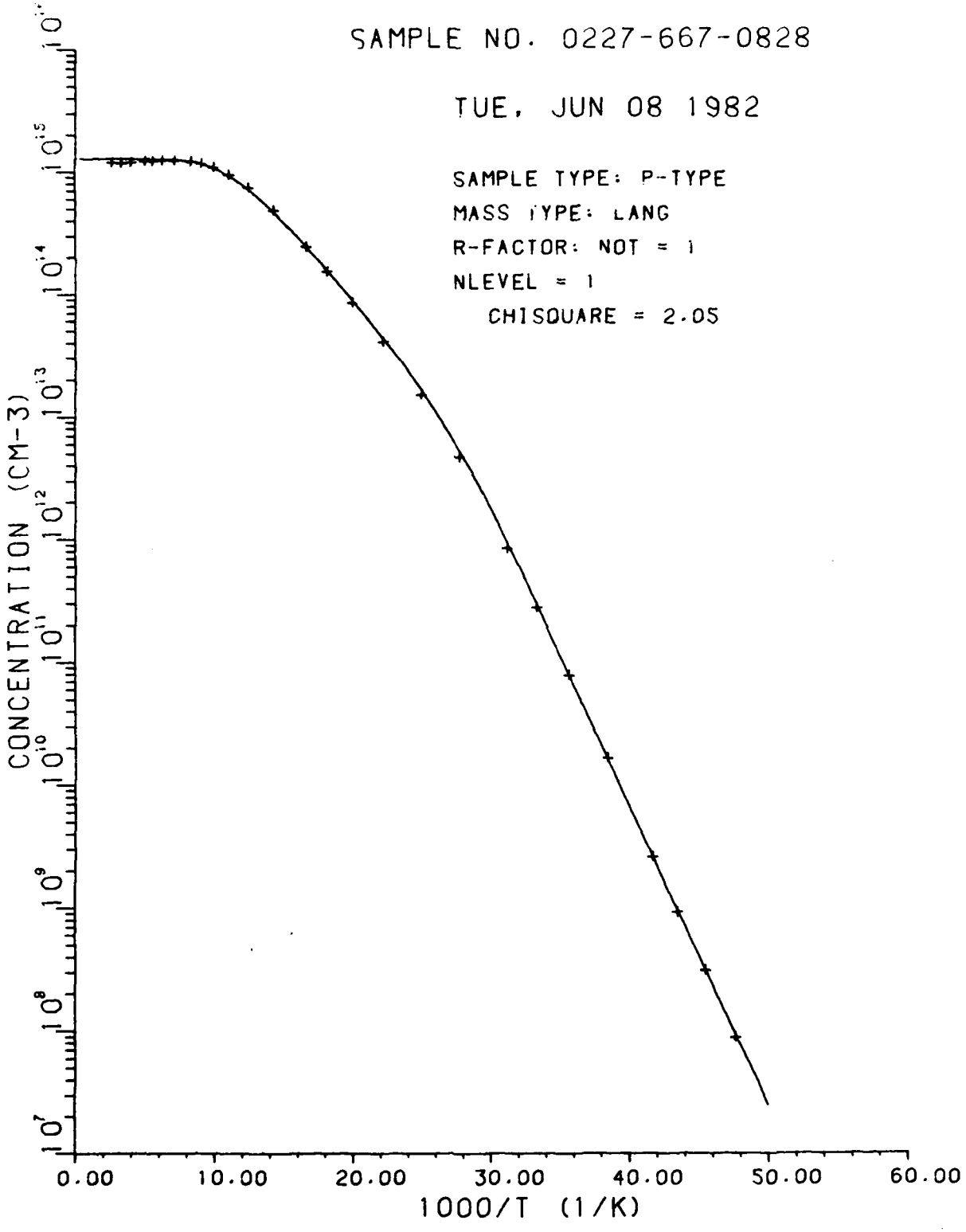

Figure 5. One Level Fit of Carrier Concentration Data vs. 1000/T for Sample 0227-667-0828.

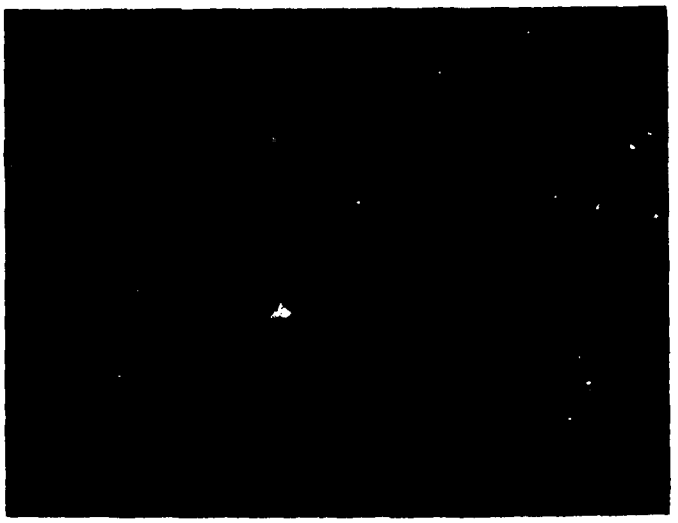

a. Crystal 1. 50 μm

b. Crystal 6. 50 μm

Figure 6. Comparison of Types of Defects Observed in Crystal 1 and Crystal 6 After Wright Etching.

TABLE 1

FUTURE SILICON MATERIALS REQUIREMENTS COMPARED TO TYPICAL CURRENT MATERIAL[a]

PROPERTY	CURRENT CZOCHRALSKI	CURRENT FLOAT ZONE	REQUIREMENTS
RESISTIVITY n-TYPE (PHOSPHORUS)	1-50 ohm-cm	1-1000 ohm-cm	100-400 ohm-cm
RESISTIVITY p-TYPE (BORON)	0.005-50 ohm-cm	1-1000 ohm-cm	100-400 ohm-cm
RESISTIVITY GRADIENT n-TYPE	3% min.	20% min.	<1%
RESISTIVITY GRADIENT p-TYPE	10% min.	20% min.	<1%
RESISTIVITY MICROSEGREGATION	3-15%	20-50%	<1%
MINORITY CARRIER LIFETIME	30-300 μs	1000 μs	300-1000 μs
OXYGEN CONCENTRATION	5-25 ppma	not detected	uniform and controlled
CARBON CONCENTRATION	1-5 ppma	<0.01-1 ppma	<0.1 ppma

[a]This Table adapted from Table 5.1 of Solid State Sciences Committee report on "Microstructure Science, Engineering, and Technology" published by National Academy of Sciences, 1979.

TABLE 2

LOWER DETECTION LIMITS IN FTIR SPECTROSCOPY FOR IMPURITIES IN SILICON
(T = 20°K, sample thickness = 4 mm)

IMPURITY	LOWER LIMIT ATOMS/cm^3	PPMA
CARBON	mid 10^{15}	0.1
OXYGEN	mid 10^{14}	0.01
BORON	mid 10^{11}	0.00001
PHOSPHORUS	mid 10^{11}	0.00001

Note: 1ppma = 5×10^{16} atoms/cm^3

TABLE 3

FTIR RESULTS FOR SOME COLD CRUCIBLE SILICON SAMPLES
AND POLY SILICON STARTING MATERIALS (ND = NOT DETECTED)

CRYSTAL SEQUENCE NO.	AFWAL/MLPO SAMPLE NO.	RADC SAMPLE NO.	OXYGEN (atoms/cm^3)	CARBON (atoms/cm^3)	BORON (atoms/cm^3)
1	0205-523-0762	---	ND	1.0×10^{17}	ND
2	0206-526-0767	Si-47	5.2×10^{15}	1.1×10^{17}	4.0×10^{14}
3	0224-657-0821	93S	2.3×10^{15}	3.6×10^{16}	1.4×10^{15}
4	0225-660-0823	93T	2.1×10^{15}	3.4×10^{16}	1.5×10^{15}
5	0226-663-0825	103S	1.8×10^{15}	2.2×10^{17}	1.5×10^{15}
6	0227-666-0827	103T	1.7×10^{15}	1.6×10^{17}	1.6×10^{15}
	0204-522-0760	poly Si (HEMLOCK#021271)	ND	9.2×10^{16}	ND
	0200-482-0699	poly Si #CB078189	ND	8.0×10^{16}	7×10^{13}

TABLE 4

SOME PUBLISHED VALUES OF IR ABSORPTION CALIBRATION FACTORS FOR CARBON AND OXYGEN IN SILICON

IMPURITY	CALIBR. FACTOR[a] (atoms/cm^3)	CALIBR. FACTOR[a] (ppm atomic)	SOURCE	TEMP.
CARBON	1.1×10^{17}	2.2	ASTM-F123-74	300K
	4.0×10^{16}	0.8		78K
	3.1×10^{16}	0.6	Hughes	78K
	8.8×10^{16}	1.8	Honeywell	78K
	6.7×10^{16}	1.3		4-20K
	7.8×10^{16}	1.6	U.D.R.I.	10K
OXYGEN	4.8×10^{17}	9.63	ASTM-F121-76	300K
	2.4×10^{17}	4.81	(old standard)	78K
	2.45×10^{17}	4.9	ASTM-F121-80	300K
	0.95×10^{17}	1.9	(new standard)	78K
	1.4×10^{17}	2.8	Hughes	78K
	8.5×10^{16}	1.7	Honeywell	78K
	3.1×10^{16}	0.6		4-20K
	2.5×10^{17}	4.9	Graff et al.	300K
	9.5×10^{16}	1.9		78K
	1.2×10^{17}	2.4	U.D.R.I.	10K
	3.0×10^{17}	6.0	Shin-Etsu Handotai	300K

[a]Concentration = peak absorption coefficient (α) X calibration factor.

TABLE 5

HALL RESULTS FOR COLD CRUCIBLE SILICON SAMPLES

CRYSTAL SEQUENCE NO.	AFWAL/MLPO SAMPLE NO.	RADC SAMPLE NO.	NET DONORS (atoms/cm^3)	BORON (atoms/cm^3)
1	0205-523-0765	---	4.5×10^{13}	7.0×10^{14}
2	0206-525-0766	Si-47	3.5×10^{13}	7.4×10^{14}
3	0224-525-0822	93S	1.3×10^{13}	1.2×10^{15}
4	0225-772-0966	93T	1.5×10^{13}	1.4×10^{15}
5	0226-664-0826	103S	4.7×10^{13}	1.3×10^{15}
6	0227-667-0828	103T	1.2×10^{13}	1.3×10^{15}

TABLE 6

RESISTIVITY AND HALL MOBILITY AT 300K FOR COLD CRUCIBLE SILICON SAMPLES

CRYSTAL SEQUENCE NO.	AFWAL/MLPO SAMPLE NO.	RADC SAMPLE NO.	RESISTIVITY (ohm-cm)	HALL MOBILITY (cm^2/volt-sec)
1	0205-523-0765	---	21.9	348
2	0206-525-0766	Si-47	20.8	320
3	0224-658-0822	93S	13.7	295
4	0225-772-0966	93T	11.9	316
5	0226-664-0826	103S	12.3	318
6	0227-667-0828	103T	12.3	317

TABLE 7

DEFECT DENSITIES IN COLD CRUCIBLE SILICON SAMPLES

CRYSTAL SEQUENCE NO.	AFWAL/MLPO SAMPLE NO.	RADC SAMPLE NO.	DISLOCATION DENSITY (cm^{-2})	STACKING FAULT AND OTHER DEFECT DENSITY (cm^{-2})	TOTAL DEFECT DENSITY (cm^{-2})
1	----	----	3.9×10^4	6.8×10^2	4.0×10^4
2	0206-527	Si-47	5.0×10^3	5.4×10^2	5.6×10^3
3	0224-659	93S	1.3×10^3	4.7×10^3	6.0×10^3
4	0225-662	93T	4.6×10^3	3.5×10^3	8.1×10^3
5	0226-665	103S	5.8×10^2	4.7×10^3	5.3×10^3
6	0227-668	103T	2.3×10^3	1.2×10^4	1.4×10^4


ATE
LME